

Supporting Information

Efficient Second-Order Nonlinear Response and Upconversion Emission from Wide-Bandgap Quasi-1D Lead Bromide Perovskite

Yun-ke Zhou^a, Wanning Li^b, Xiao-mei Chen^a, Xiao-Ze Li^a, Xiao-Jie Wang^a, Benfeng Bai^{*a}, Yu Chen^{*b}, Hong-Hua Fang^{*a}

^a State Key Laboratory of Precision Measurement Technology and Instruments, Department of Precision Instrument, Tsinghua University, Beijing 100084, P. R. China. E-mail: hfang@mail.tsinghua.edu.cn, baibenfeng@tsinghua.edu.cn

^b MIIT Key Laboratory for Low-Dimensional Quantum Structure and Devices, School of Materials Science and Engineering, Beijing Institute of Technology, Beijing 100081, P. R. China. E-mail: chenyubit@bit.edu.cn.

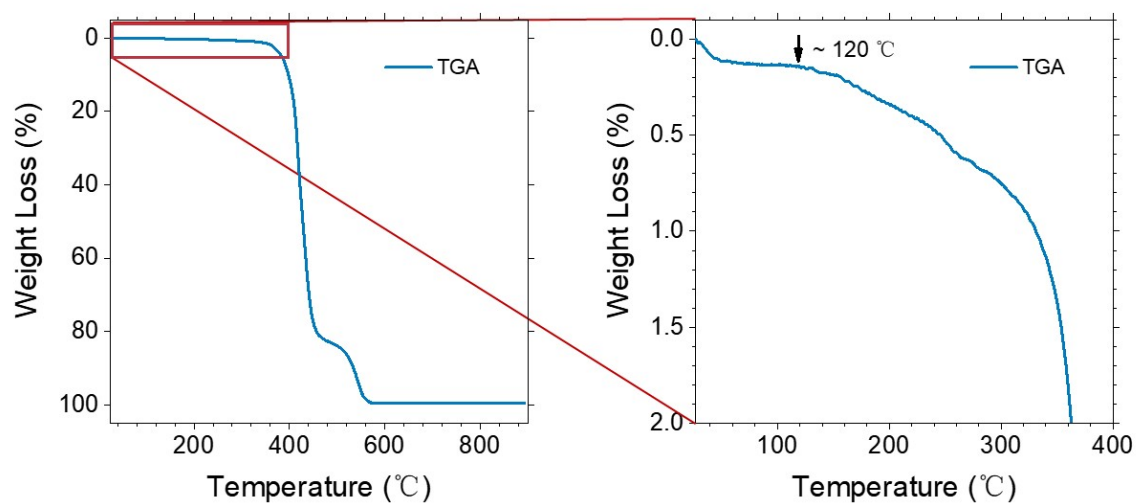


Figure S1. Left panel: Thermal gravimetric analysis (TGA) plots for $\text{PEA}_3\text{PbBr}_5 \cdot \text{H}_2\text{O}$ crystals. Right panel: The corresponding region as marked with a red rectangular.

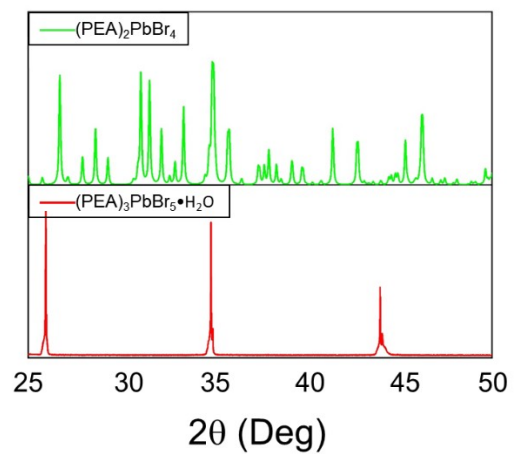


Figure S2. Simulated XRD patterns of $\text{PEA}_3\text{PbBr}_5 \cdot \text{H}_2\text{O}$ and $\text{PEA}_2\text{PbBr}_4$ crystals.

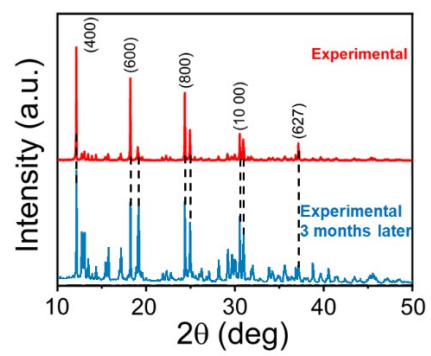


Figure S3. Comparison of measured powder X-ray diffraction (PXRD) diagram of PEA3PbBr5 crystals over three months.

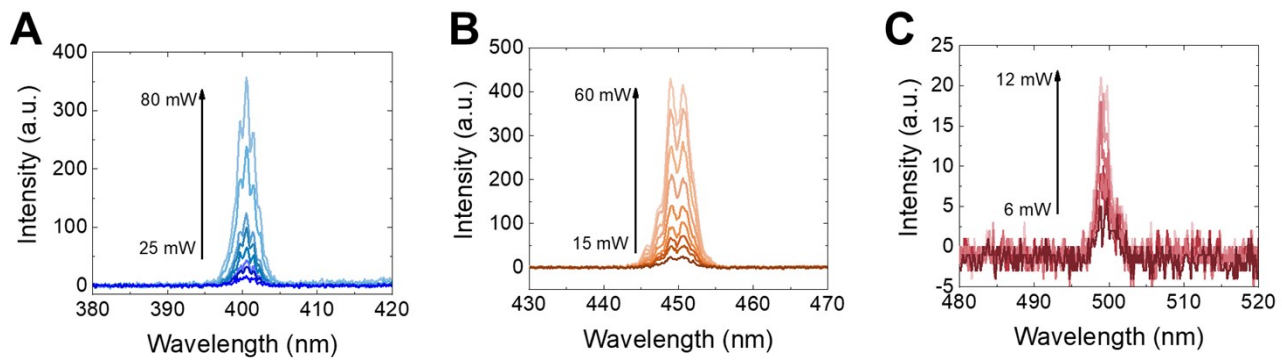


Figure S4. The power-dependent SHG plots excited at different wavelengths, A) 800 nm, B) 900nm, and C) 1000 nm.

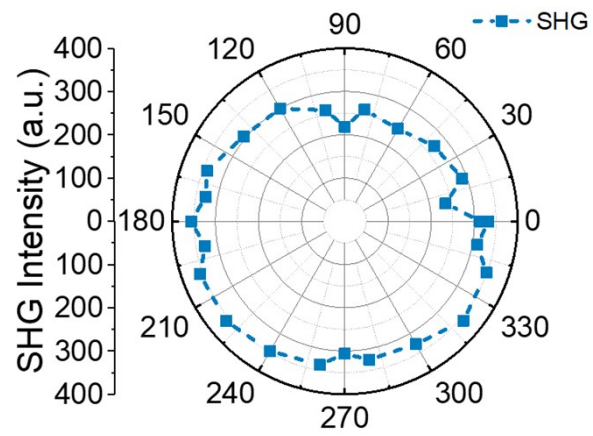


Figure S5. Polar plot of SHG intensity as a function of excitation polarization angle θ .

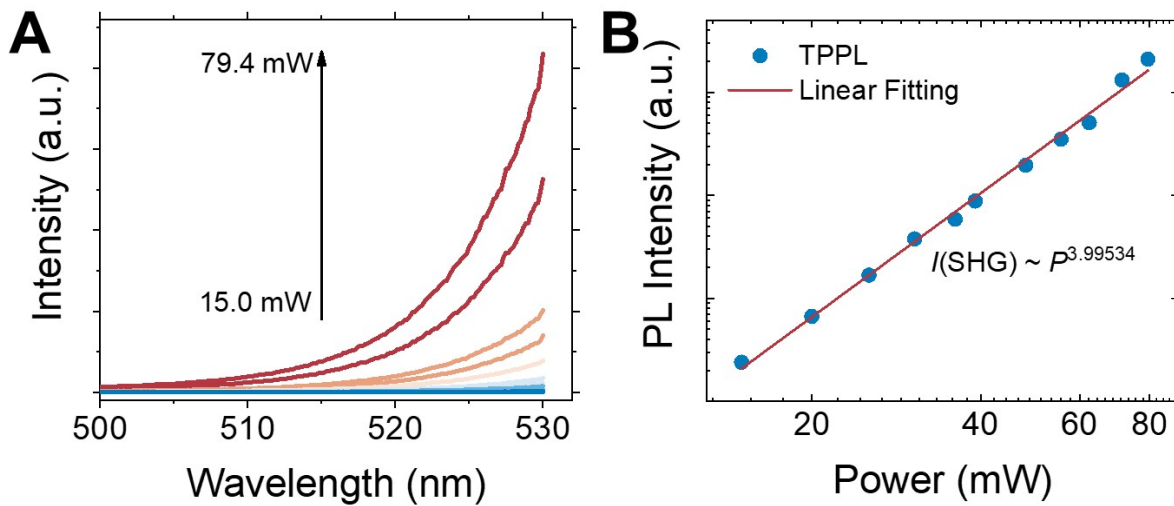


Figure S6. A) Power-dependent TPPL spectra at the excitation wavelength 800 nm with various power from 15.0 mW to 79.4 mW. B) Logarithmic diagrams of the power-dependent TPPL intensity corresponding to the spectra in A).

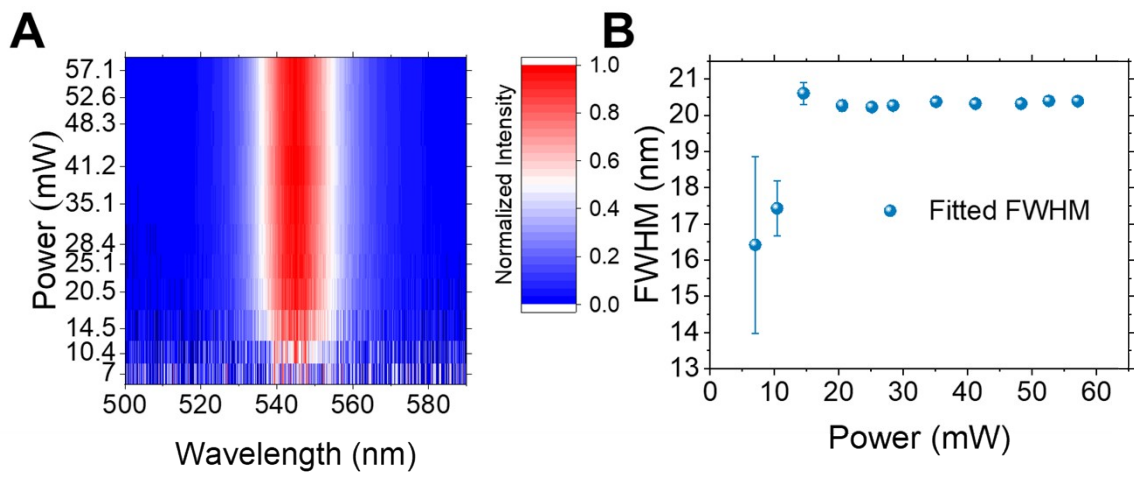


Figure S7. A) Normalized spectral- and power-dependent PL images at the excitation wavelength of 900 nm with various power from 7 mW to 57.1 mW. B) Gaussian fitted full-width of half maximum (FWHM) as a function of power density.

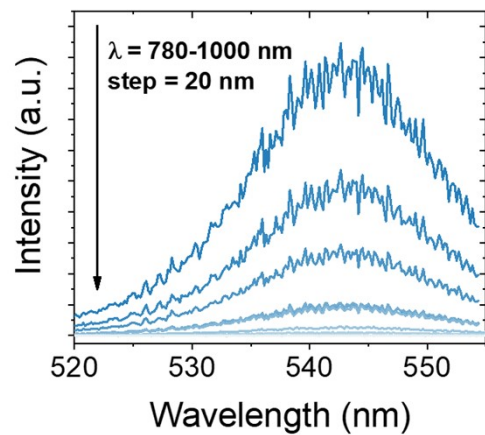


Figure S8. Wavelength-dependent TPPL spectra at the excitation wavelength varying from 780 to 1040 nm with a step of 20 nm.

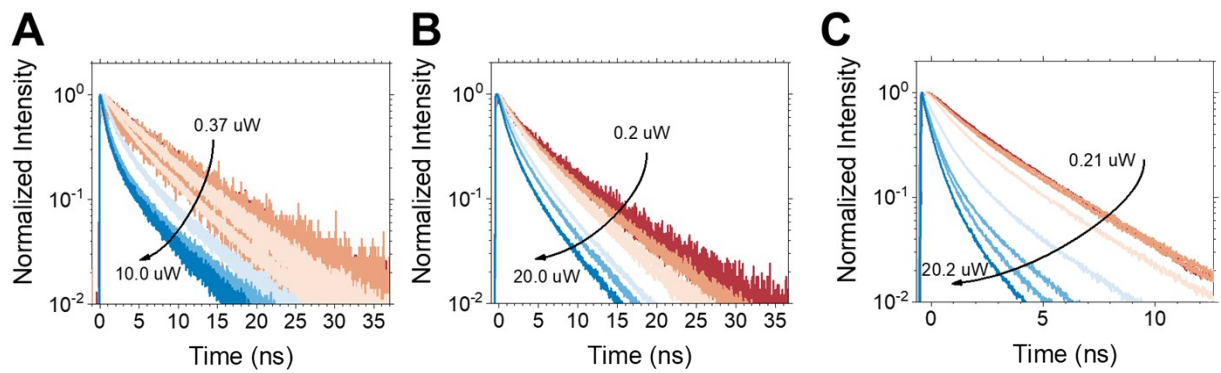


Figure S9. A-C) Excitation power-dependent PL dynamics at different positions excited by a femtosecond pulsed laser at 400 nm.

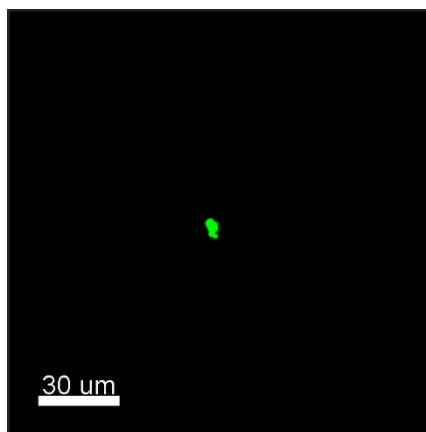


Figure S10. Photoluminescence image with wide-field UV (330 nm - 380 nm) LED illumination.
Scale bar: 30 μm .

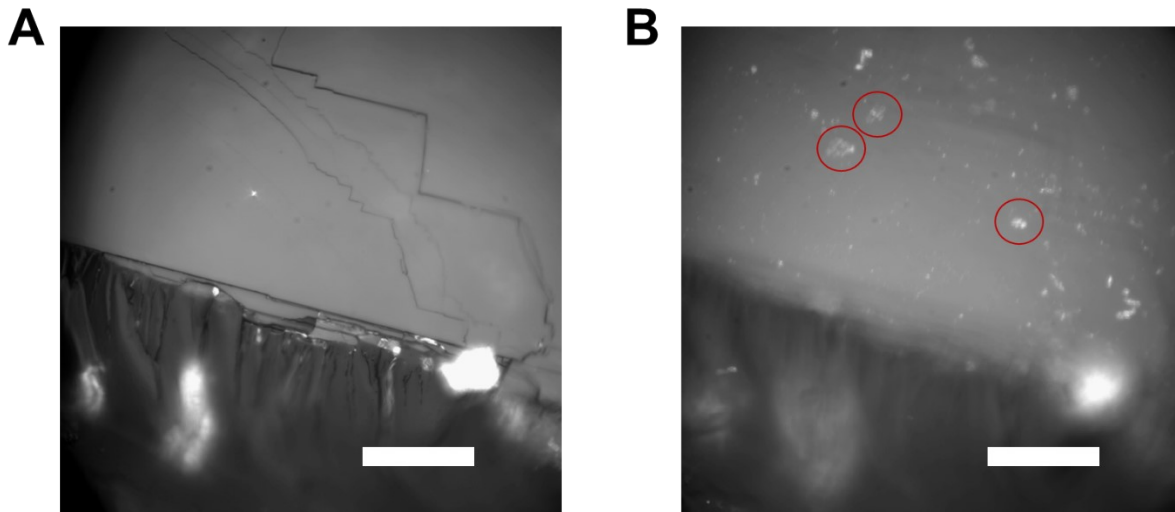


Figure S11. A-B) Photograph of the PEA₃PbBr₅·H₂O single-crystal captured by a monochrome CMOS camera with wide-field blue LED illumination. A) Surface. B) Interior. Scale bar: 20 μm.

Table S1: Crystallographic data for PEA₃PbBr₅·H₂O single-crystal.

Formula	(PEA) ₃ PbBr ₅ ·H ₂ O
Formula weight	987.7
Temperature (K)	Room temperature (296)
Crystal system	monoclinic
Space group	C2/c
a (Å)	29.269(3)
b (Å)	8.1369(7)
c (Å)	27.879(2)
α	90.0000
β	92.448(2)
γ	90.0000
Unit-cell volume (Å ³)	6633.6 (10)
Z	8
Z'	1
Density (calculated) / (g·cm ⁻³)	1.985
F000	3744
μ (mm ⁻¹)	11.130
Wavelength (Å)	0.71073
Data completeness	0.991
R (reflections)	0.0372 (3843)
wR2 (reflections)	0.1108 (5822)
S	0.836

Table S2: Comparison of second-order nonlinear behavior of lead halide perovskites.

Composition	Morphology	Optical gap (eV)	λ (nm)	$\chi^{(2)}$ (pm/V)	Ref
PEA ₃ PbBr ₅ ·H ₂ O	Single crystals	4.20	900	0.1	This work
(R-MPEA) _{1.5} PbBr _{3.5} (DMSO) _{0.5}	Nanowires	3.07	850	0.68	1
(PMA) ₂ PbCl ₄	Single crystals	3.65	1550	1.4	2
(C ₅ H ₁₃ N ₂) PbCl ₄ ·H ₂ O	Single crystals	3.80	1064	0.32	3
(2-FBA) ₂ PbCl ₄	Single crystals	3.62	1064	0.35	4

References

1. C. Yuan, X. Li, S. Semin, Y. Feng, T. Rasing and J. Xu, *Nano Lett.*, 2018, 18, 5411-5417.
2. Y. Gao, G. Walters, Y. Qin, B. Chen, Y. Min, A. Seifitokaldani, B. Sun, P. Todorovic, M. I. Saidaminov, A. Lough, S. Tongay, S. Hoogland and E. H. Sargent, *Adv. Mater.*, 2019, 31, e1808336.
3. Y. Peng, Y. Yao, L. Li, Z. Wu, S. Wang and J. Luo, *J. Mater. Chem. C*, 2018, 6, 6033-6037.
4. P. P. Shi, S. Q. Lu, X. J. Song, X. G. Chen, W. Q. Liao, P. F. Li, Y. Y. Tang and R. G. Xiong, *J. Am. Chem. Soc.*, 2019, 141, 18334-18340.